Int J Adv Manuf Technol (2015) 80:1713–1720
DOI 10.1007/s00170-015-7145-8

ORIGINAL ARTICLE

Ablation and morphological evolution of micro-holes in stainless steel with picosecond laser pulses

Wanqin Zhao[1,2] · **Wenjun Wang**[1] · **Gedong Jiang**[1] · **Ben Q. Li**[2] · **Xuesong Mei**[1]

Received: 12 February 2015 / Accepted: 12 April 2015 / Published online: 24 April 2015

Abstract An experimental study is presented of micro-hole drilling on the surface of stainless steel using a 10-ps Q-switched Nd:VAN pulsed laser at two wavelengths, 532 and 1064 nm, with multiple powers and different number of pulses. Results show that two primary ablation mechanisms for ultrashort laser machining, i.e., vaporization and phase explosion, which correspond to gentle and strong ablations, are correlated mainly with the applied laser power. From measured data, two ablation thresholds are calculated using a piece-wise linear fitting. Moreover, surface recast layer associated with strong ablation can be eliminated by an appropriate selection of laser processing parameters. The Hirschegg model is applied to analyze the evolution of hole depth as a function of laser processing parameters for the two wavelengths. For the 532-nm wavelength laser ablation, the shapes and morphology of micro-holes evolve differently with low power from high power. In addition, the related reasons inducing multiple featured hole shapes are discussed.

Keywords Ablation · Evolution · Stainless steel · Picosecond laser

✉ Wenjun Wang
wenjunwang@mail.xjtu.edu.cn

[1] State Key Laboratory for Manufacturing Systems Engineering, Xi'an Jiaotong University, Xi'an 710049, China

[2] Department of Mechanical Engineering, University of Michigan, Dearborn, MI 48128, USA

1 Introduction

Ultrashort laser machining has received considerable attention since its invention due to its unique advantages, and nowadays, it is a tool of choice for precision removal of material. Ultrashort laser, including low picosecond and femtosecond lasers, has a short pulse duration and delivers high peak power. In comparison to low picosecond lasers, femtosecond lasers are complex, expensive, and of low repetition rate. These drawbacks have limited the widespread use of femtosecond lasers for practical industrial applications [1, 2]. In general, laser machining may operate in one of three distinctive modes, depending upon the pulse duration, as shown in Fig. 1 [3, 4]. For a pulse duration of an order of sub picosecond, cold ablation dominates, during which nonlinear effects (e.g., filamentation) occur as a result of the interaction of ultrashort laser with air in the laser-focal region. These nonlinear effects can be detrimental, leading to poor machining quality. For a pulse duration in the range of a few nano to microseconds, thermal effects and incidental melt expulsion come into play, giving rise to a large heat-affected zone and an extended recast layer. Hot ablation becomes operative when a pulse duration is tuned within the low range of picoseconds. Experience suggests that hot ablation with a pulse duration ranging between 5 and 10 ps is optimal for machining of micro-sized holes in metals [5–8].

In recent years, several groups have demonstrated that laser wavelength can be an important processing parameter for drilling of micro-holes in metals using a low picosecond laser. It was found that by use of a 10-ps laser with same fluences and focus radius, a deeper hole and/or a hole with a larger aspect ratio was ablated in stainless steel with a wavelength of 532 nm than 1064 nm in our previous study [9]. Tunna et al. reported that the highest average drilling rate of ablation with a wavelength of 1064 nm was much smaller than that with

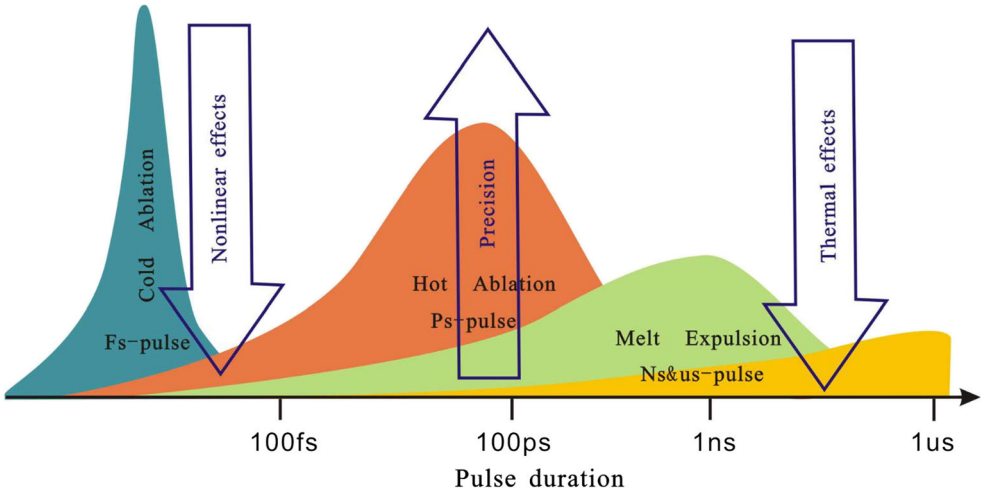

Fig. 1 Illustration of three different physical domains with respect to the pulse duration

either 532 or 355 nm. The average drilling rates, however, were similar for 532 and 355 nm, because chromium in 316L stainless steel formed a pacifying oxide layer, which prevented corrosion from occurring on the surface [10]. Spiro et al. showed that a UV picosecond laser had a higher processing rate than a near-IR femtosecond laser for precision machining of metals [11]. Stašić et al. studied the effect of different wavelengths and found different surface features and oxygen contents with a picosecond laser on Inconel 600 super alloys [12]. However, there appears to have been no reports on the evolution of hole shape and morphology during drilling of opaque metals using a low picosecond laser with different wavelengths, despite its important implication for fundamental understanding and process optimization of low picosecond laser metal micromachining.

In this paper, experiments were carried out in stainless steel using the 10-ps laser at two wavelengths (532 and 1064 nm) for different powers and pulses, with an intent to provide an enhanced understanding of fundamentals governing the evolution of micro-hole morphology during ultrashort laser drilling. Gentle ablation and strong ablation are two primary ablation mechanisms (vaporization and phase explosion) associated with laser machining. They were characterized by a piece-wise linear fitting of experimental measurements. After samples were grinded, followed by ultrasonic cleaning, geometric shape and morphological features of micro-holes were obtained. Based on the Hirschegg model, time development of hole depth and effects of processing parameters were analyzed for each wavelength. Two ablation routes of micro-hole drilling along with multiple features of hole shapes fabricated using the 532-nm laser were presented.

2 Experiments

Stainless steel (SS304) samples were used. The laser utilized for irradiation was a neodymium-vanadate (Nd:VAN; Austria) laser delivering pulses of 10 ps in duration, 532 and 1064 nm wavelengths, 2 W of power, and a repetition rate of 1 kHz. The laser beam was linear polarization. A ×150 optical lens was used to focus the beam on the sample. After the experiments, the holes were split using sandpapers and polishing agents, and then cleaned in an ultrasonic cleaner with acetone. This procedure washed off fragments remaining after the use of sandpapers or polishing agents. At last, through various tools, such as scanning electron microscopy (SEM) and laser scanning confocal microscopy (LSCM), the authentic depth and longitudinal section of hole along with the morphology of the hole were determined.

3 Results and discussions

3.1 Hole ablation and threshold

A critical parameter for ultrashort laser micromachining is the metastable ablation threshold of the material being machined. A significant amount of research is being carried out to study the interaction between ultrashort laser and material, and it has been found that effective ablation is achieved only when laser fluence is equal to or higher than the ablation threshold. When ablation threshold is not reached, changes in chemical and structural characteristics are observed without a crater or hole being formed. An example of an ablated area is shown in Fig. 2. A comparison of Fig. 2(A and B) shows that there are some differences in the ablation morphologies. Melting of material is absent in the case of Fig. 2(A), whereas, in the case of Fig. 2(B), obvious molten materials on the surface and pinholes on the bottom are observed. This is because drilling of the two holes is by different ablation mechanisms.

For ultrashort laser, vaporization and phase explosion are the two primary ablation mechanisms which correspond to two separate ablation regimes: *gentle* ablation and *strong* ablation [13]. For the former, the material is heated and then

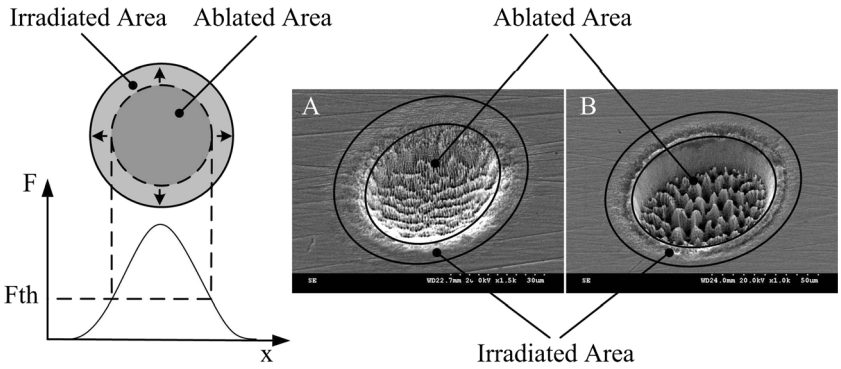

Fig. 2 Laser ablation and the threshold

removed from the material surface in vapor form. A characteristic of this mechanism is that no melting for the material occurs, as shown in Fig. 3(A). The latter is a complex ablation mechanism with the merging of liquid droplets and vapor as well as high pressure and expansion. The molten materials or recast layer on the hole surface is obvious, as shown in Fig. 3(B and C). From Fig. 3, it can be concluded that holes ablated with the same power and increasing pulses result from the same ablation mechanism. This indicates that the ablation mechanisms may be determined from the applied power and are not related to the pulses. Furthermore, recast layer is unavoidable even in the case of a femtosecond laser and is typically composed of insufficient material expulsion. It is interesting that for strong ablation, this is Fig. 3(B and C), with increasing pulses, the recast layer on the hole surface has not been increased but reduced in some regions of the drilled hole, as shown in Fig. 3(B2 and B3), or in the entire area shown in Fig. 3(C2 and C3). This occurs due to the influence of subsequent pulses on the surface recast layer, indicating that a hole with little surface recast layer can be achieved through an appropriate selection of processing parameters even for strong ablation.

In practice, ultrashort laser fabrication of micro-holes is carried out by one of the following four methods, namely the single-pulse [14], percussion [15–17], trepanning [18, 19], and helical drilling [20], and *chip* volume is found to decrease and precision is improved in order. However, each of the drilling procedures gradually increases in complexity [21]. Furthermore, the single-pulse drilling allows a small amount of material to be removed because of only one pulse. With both trepanning and helical drilling, the ablated hole diameter is limited by the diameter of the laser beam. As a result, these two methods are not used for drilling holes with a small aperture. Percussion drilling is not limited by the above factors, though it has its own limitations associated with surface recast layer and deep hole drilling. It is noteworthy that the chip volume is small but hole depth is limited for the gentle

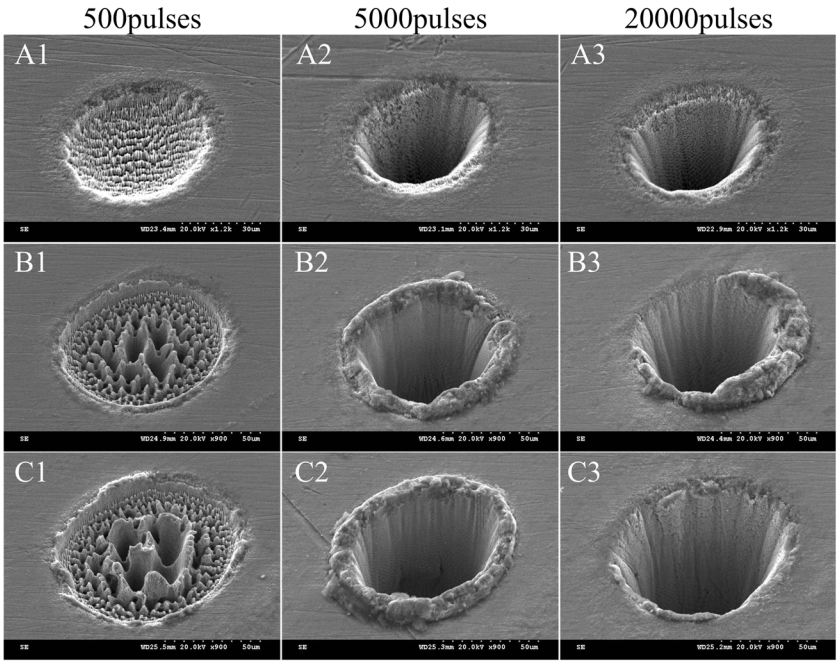

Fig. 3 SEM images of the holes ablated by the 10-ps laser at the 1064-nm wavelength (*A* 1.28 J/cm^2; *B* 6.42 J/cm^2; *C* 9.85 J/cm^2)

ablation using percussion, and strong ablation is the main processing mechanism for laser machining of high aspect ratio micro-holes. Figure 3(B3 and C3) indicates that a micro-hole with little or very minimal surface recast layer can be fabricated using percussion, which has some guiding for high-quality micro-small deep hole processing.

In addition, for gentle ablation and strong ablation, there are two ablation thresholds referred to as gentle ablation threshold and strong ablation threshold. These thresholds are among the most important characteristics for ultrashort laser ablation. Evaluation of the ablation thresholds is determined using an ultrashort laser pulse with the Gaussian beam [22–24]. The threshold is estimated from the relationship between the laser peak fluence F_0^{pk} or the pulse energy E_p and the diameter D of a hole ablated, shown in Eq. (1),

$$D^2 = 2\omega_0^2 \, ln\left(-\frac{F_0^{pk}}{F_{th}}\right) = 2\omega_0^2 \, ln\left(-\frac{E_p}{E_{th}}\right) \tag{1}$$

where ω_0 ($1/e^2$) is the laser beam radius and F_{th} is the threshold fluence. Relationship between laser peak fluence F_0^{pk} and the pulse energy E_p is given in Eq. (2),

$$F_0^{pk} = \left(\frac{2E_p}{\pi\omega_0^2}\right) \tag{2}$$

where F_0^{pk} is the fluence of the Gaussian beam when the radius is equal to zero, and the Gaussian distribution of laser fluence can be determined by Eq. (3),

$$F(r) = F_0^{pk}\exp\left(-\frac{2r^2}{\omega_0^2}\right) \tag{3}$$

Next, a logarithmic fit for the data is carried out according to the relation $D^2 \sim E_p$ based on Eqs. (1) and (2), and the slope $2\omega_0^2$ is estimated. At this point, pulse energy E_p can be transformed into the laser fluence. Another linear fitting of the data based on the relationship $D^2 \sim \ln(F_0^{pk})$ is carried out. The intercept on the horizontal axis is $\ln F_{th}$, and then upon taking anti-logarithm, the ablation threshold can be determined.

Figure 4 shows a piece-wise linear fitting for the squared crater diameters and the natural logarithm of peak fluence for the 10-ps ultrashort laser with the 500, 2000, and 10,000 pulses, respectively. For the piece-wise linear fitting, the first phase represents gentle ablation and the second is strong ablation. These are also verified from the SEM images in Fig. 4. First, for Fig. 4(A), there is little evidence of material melting occurring, indicating that vaporization is the ablation mechanism, which is nothing but the gentle ablation. On the other hand, molten materials on the surface and pinholes on the bottom are obvious in Fig. 4(B–D); this indicates that phase explosion or strong ablation is the ablation mechanism.

Then, based on an empirical incubation model [25], the relationship between threshold fluence $F_{th}(N)$ for N laser pulses and single-shot ablation threshold fluence $F_{th}(1)$ are related by the following Eq. (4),

$$F_{th}(N) = F_{th}(1)N^{S-1} \tag{4}$$

where S is the incubation coefficient that describes incubation occurring in the material after laser irradiation and can be calculated. Specifically, Eq. (4) is transformed into the following Eq. (5),

$$\ln(N \cdot F_{th}(N)) = \ln F_{th}(1) + S \cdot \ln N \tag{5}$$

Based on Eq. (5), a linear fit of the data is performed, as shown in Fig. 5, according to the relation $\ln(N \cdot F_{th}(N)) \sim \ln N$. The slope of the fitting line is S and intercept at the vertical axis is $\ln F_{th}(1)$. Therefore, the incubation coefficient S and the single-shot ablation threshold fluence $F_{th}(1)$ are 0.858 and 0.276 J/cm^2 for the gentle ablation and 0.987 and 2.537 J/cm^2 for the strong ablation.

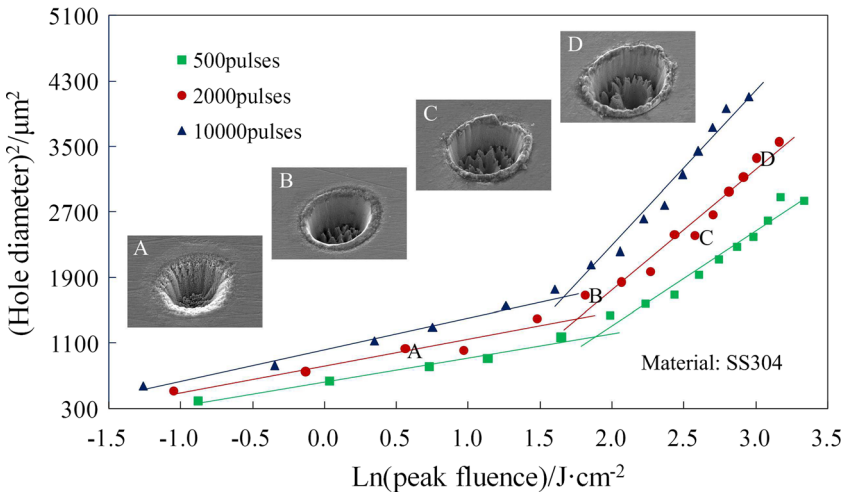

Fig. 4 Linear fit for crater diameters squared and natural logarithm of peak fluence (*A–D* SEM images of the holes ablated by the 10-ps laser with different fluences and the same number of pulses of 2000)

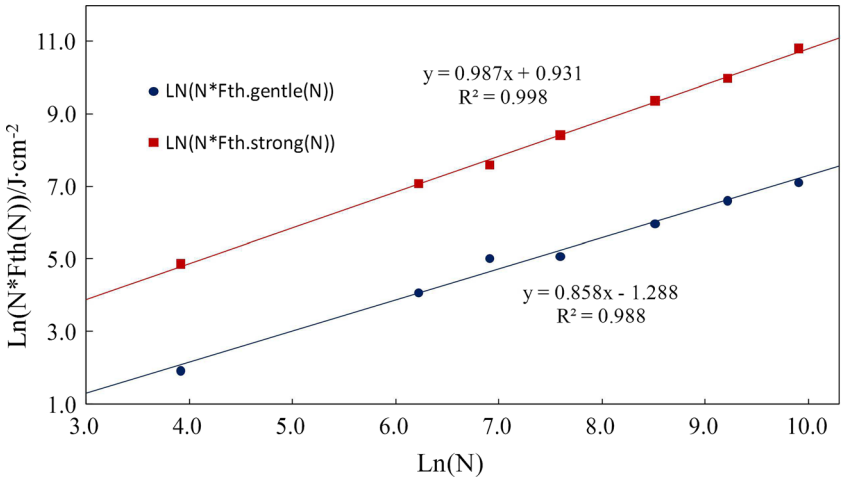

Fig. 5 Curves for incubation effect (the *solid line* represents the linear fit according to Eq. (5))

3.2 Evolution of hole morphology

Based on the above discussion, an appropriate combination of powers and number of pulses is critical in control of machining quality. The Hirschegg model, established in the late twentieth century, is a well-known method that allows a description of depth evolution for ultrashort laser machining [26]. The main principles taken into consideration are the laser beam and the laser-induced plasma. The laser beam is primarily responsible for increasing the depth of the hole in the propagation direction of a laser beam. The laser-induced plasma allows the removal of material along the radial direction, thereby widening the hole and smoothing the wall surface. Based on the Hirschegg model, evolution of the hole depth is divided into four phases [27]. In phase I, ablation starts with the highest drilling rate and the surface is almost fat. During phase II, a capillary is formed with a large decrease in ablation rate. Next, in phase III, a deep hole is drilled into the material and ablation rate further decreases. Finally, in phase IV, ablation stops suddenly, without further decrease in ablation rate. Based on this model, evolution of the hole depths at two different wavelengths, 532 and 1064 nm, with different powers and pulses on the surface of stainless steel can be characterized. Influences of parameters will be analyzed in the following sections.

3.2.1 Evolution of hole depth

Figure 6 shows evolution of hole depth and ablation rate as a function of applied pulses at the 532-nm wavelength. Apparently, ablations for powers of 7 and 72 mW with the pulses from 50 to 20,000 completely go through all phases of the Hirschegg model, whereas, for a much higher power of 112 mW, all phases are not completed and ablation is still in phase III with 20,000 pulses. Furthermore, the ablation rate decreases with the increasing number of pulses and the decreasing in laser power.

It is noted that from Fig. 6, the depth of holes shows a small difference between different powers of 72 and 112 mW with the same number of pulses except with the pulses of 20,000. Here, ablation for 72 mW has saturated and reaches a steady state, and an increase in powers does not change the hole depth. However, the hole depth experiences a continuous increase for 112 mW with the pulses of 20,000 and the hole depth evolution is in phase III. It is perhaps reasonable to suggest that there is a constraint relationship between power and number of pulse to reach hole depth saturation.

To further explore this relationship between the power and the number of pulse, additional experiments with much higher powers and more pulses at the 1064-nm wavelength were carried out. Results from these experiments are summarized in Fig. 7. Due to the more initial pulses (i.e., 2000), ablation is in phase III for both 112 and 212 mW. For 72 mW, the ablation is in phase III and phase IV. Meanwhile, similar phenomena are observed in Figs. 6 and 7. For instance, when the number of pulses is less than 10,000, hole depth reaches a saturation state for 72 mW. Thus, for similar hole depths obtained with 72 mW and higher powers 112 and 212 mW, only a small fluctuation in the ablation rates is seen before reaching saturation. With the number of pulses increasing, ablation with 72 mW is into phase IV, whereas with the other two powers, ablation is still in phase III. With pulse number increasing from 10,000 to about 40,000, another saturation state is seen for ablation at 112 and 212 mW. Increasing the number of pulses further results in the overcoming of the saturation state and hole depth continues to increase for higher power, with 212 mW yielding a higher increase than 112 mW.

Overall, the phenomenon abovementioned illustrates that the higher the power, the more the saturation pulses, namely the amount of saturation pulses is defined in terms of the applied power. Additionally, it can be seen that there is a range of pulse within which the power is saturated and further increasing the laser power would not drill a deeper hole. Moreover, as the number of pulses continues to increase, this

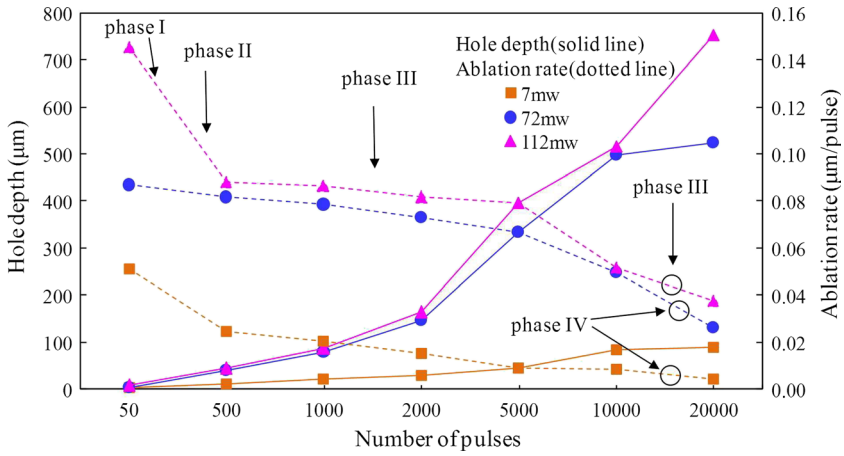

Fig. 6 Hole depth and ablation rate versus the number of pulses at the 532-nm wavelength

saturated state is overcome with higher powers, which results in another pulse section corresponding to a higher saturation power, namely power saturation is observed in stages depending on the number of pulses.

A comparison of Fig. 6 with Fig. 7 reveals that hole depth increases, whereas ablation rate decreases to saturation gradually with the increasing number of pulses and powers at both the 532- and 1064-nm wavelengths. Meanwhile, hole depth and ablation rate are higher at 532 nm compared to 1064 nm for the same power and number of pulses. Some physical mechanisms related to wavelength, such as laser-induced plasma, are thought to be responsible for these observed phenomena.

For metal ablation, laser pulse energy is absorbed by free electrons on a femtosecond time scale [28]. On a time scale of several picoseconds, electrons are emitted from the target surface by photoelectric and thermionic effects [29, 30]. This results in the generation of the plasma plume with a delay of 5–10 ps after irradiation starts [31]. The plasma is important even in cases where ultrashort laser pulses are used. Under these influences, ablation rate is associated with energy transferring to the bottom of the hole, which is lower for 1064 nm. This is due to the stronger absorption of laser-induced plasma at 1064 nm than 532 nm [32]. As a result, ablation rate and hole depth are lower at 1064 nm in comparison with 532 nm for the same power and number of pulses. Then, plasma density reaches and exceeds the critical density with ablation; the plasma shielding develops and reflects the part of the incoming pulse, thereby causing the ablation rate to decline further and eventually stop [9, 33]. On the other hand, energy absorbed by the plasma acts as the broad of aperture and the smooth of side wall based on the Hirschegg model, and these effects become stronger with laser wavelength increasing [34]. For the wavelength effect, some experimental results have been reported in literature; for example, when 532 nm is used instead of 1064 nm, channel tip appears narrower [32] and the side wall is rough [35].

3.2.2 Evolution of hole morphology

Through grind cleaning, evolution of the longitudinal section of holes ablated at the 532-nm wavelength was obtained, and the results are shown in Fig. 8. Each row shows holes ablated with a different number of applied pulses and other parameters kept constant. When the power is low (e.g., 7 mW), the hole morphology evolves from a shallow crater to a conical hole,

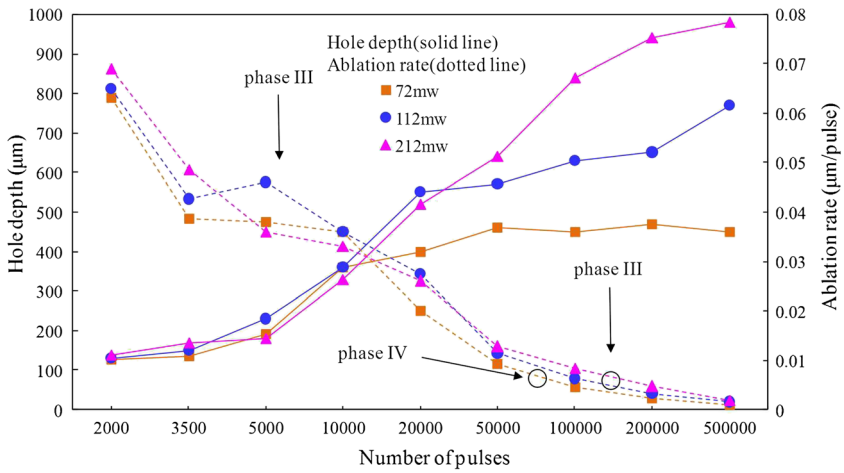

Fig. 7 Hole depth and ablation rate versus the number of pulses at the 1064-nm wavelength

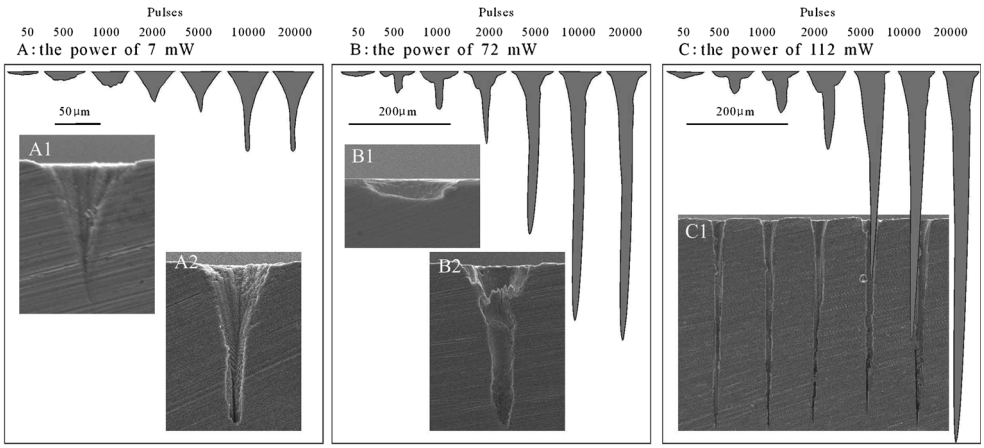

Fig. 8 Evolution of the longitudinal section of hole ablated by the 10-ps laser at the 532-nm wavelength (*A1*, *A2*, *B1*, *B2*, and *C1* SEM images of some featured holes shapes)

and then to a funnel-shaped hole, as shown in Fig. 8(A). The two typical shapes of holes, that is, the conical hole and funnel-shaped hole, are shown in Fig. 8(A1 and A2). Second, for a higher power (e.g., 72 and 112 mW), the hole morphology develops from a shallow crater to a papilla shape and finally to a deep channel. The typical shapes of holes are illustrated in Fig. 8(B1, B2, and C1); they are the shallow crater, papilla-shaped hole, and deep channel, respectively.

It is worth noting that the side wall surfaces of holes are characterized by ripples due to the influence of the linear polarization [36]. For percussion drilling, polarization also affects the exit shape of through-hole or derivation of blind-hole tip from the laser beam axis [37]. For blind-hole ablation in our experiments, the derivation is not observed. From this, it may be concluded that the deviation does not occur in all cases. Overall, polarization effect, both linear polarization and circular polarization, on the hole shape and morphology is certainly a good subject for further studies.

Moreover, some related reasons which induce these typical hole shapes need to be discussed. First, the shallow crater is the first stage of ablation, as shown in Fig. 8(B1). During drilling, the radiated area changes from plane to curved surface, because of a few pulses, reflection of beam is limited and not more than once, a shallow hole is produced [38]. Then, the shorter Rayleigh length at the 532-nm wavelength may be responsible for the conical hole, as shown in Fig. 8(A1). Multiple reflections, which mainly affect the concentration of energy in the center of the hole resulting in a deep and wide hole tip, are associated with the funnel-shaped hole [39], as shown in Fig. 8(A2). The conical emission which causes the beam profile to widen and distort is the principal reason for the papilla-shaped hole [40], as shown in Fig. 8(B2). Finally, deep channel with aspect ratios greater than 10 could be obtained, as shown in Fig. 8(C1).

Precise control during ultrashort laser micro-hole drilling can be achieved through the study on the evolution of holes. Higher power and number of pulses should be chosen to obtain high aspect ratio micro-hole which may be used in processing of fuel-injection nozzles and cooling channels in turbine blade. Moreover, multiple featured hole shapes discussed in this section can be used to further expand application of holes ablated by ultrashort lasers. For example, the shallow craters could be as the substrate for cell cultures or to tune the surface texture to obtain special surface characteristics, such as super hydrophobic surface, super absorbance, etc. Funnel-shaped holes can be used in filtering application as channels, which allow only some particulates to pass.

4 Conclusions

Drilling of micro-holes in stainless steel using the 10-ps Q-switched Nd:VAN pulsed laser (Austria) at two wavelengths, 532 and 1064 nm, and with multiple powers and number of pulses has been studied experimentally. It is found that the two primary ablation mechanisms of ultrashort lasers, vaporization and phase explosion, are primarily determined by the applied power. For the processing conditions considered, the two ablation thresholds are calculated through a piece-wise linear fitting of experimental data. For strong ablation, surface recast layer can be eliminated by an appropriate selection of parameters. Samples were grinded and followed by ultrasonic cleaning, and geometric and morphological features of micro-holes were characterized. Evolution of hole depth and effects of processing parameters were analyzed for two wavelengths using the Hirschegg model. Results show that ablation rate (μm/pulse) decreases with an increase in the number of pulses, while increasing with laser powers increased. Power saturation is observed in stages depending on the number of pulses. The time development of micro-hole shapes, as being ablated at the 532-nm wavelength, is found to take the following two routes: from a shallow crater to a conical hole and then to a funnel-shaped hole for low power, and from a shallow crater to a papilla shape and finally to a deep channel for high power.

Acknowledgments This work was supported by National Natural Science Foundation of China (Grant no. 51475361), Program for Changjiang Scholars and Innovative Research Team in University (Grant no. IRT1172) and China Scholarship Council (CSC).

References

1. Nebel A, Herrmann T, Henrich B, Knappe R (2005) Fast micromachining using picosecond lasers. Proc SPIE 5706:87–98
2. Cheng J, Perrie W, Sharp M, Edwardson SP, Semaltianos NG, Dearden G, Watkins KG (2009) Single-pulse drilling study on Au, Al and Ti alloy by using a picosecond laser. Appl Phys A 95: 739–746
3. Dausinger F, Hügel H, Konov VI (2003) Micro-machining with ultrashort laser pulses: from basic understanding to technical applications. Proc SPIE 5147:106–115
4. Schulz W, Eppelt U, Poprawe R (2013) Review on laser drilling I. Fundamentals, modeling, and simulation. J Laser Appl 25:012006–1–17
5. Raciukaitis G, Brtkas M (2004) Micro-machining of silicon and glass with picosecond lasers. Proc SPIE 5662:717–721
6. Ostendorf A, Kamlage G, Klug U, Korte F, Chichkov BN (2005) Femtosecond versus picosecond laser ablation. Proc SPIE 5713:1–8
7. Karnakis D, Rutterford G, Knowles M, Dobrev T, Petkov P, Dimov S (2006) High quality laser milling of ceramics, dielectrics and metals using nanosecond and picosecond lasers. Proc SPIE 6106: 610604–1–11
8. Lleinbauer J, Knappe R, Wallenstein R (2005) A powerful diode-pumped laser source for micro-machining with ps pulses in the infrared, the visible and the ultraviolet. Appl Phys B 80:315–320
9. Zhao WQ, Wang WJ, Jiang GD, Mei XS, Liu B (2014) Improving the efficiency of picosecond laser micromachining of stainless steel. Radiat Eff Defect Solid 169:102–108
10. Tunna L, Khan A, O'Neill W, Sutcliffe CJ (2006) The effect of processing wavelength and fluence on the microdrilling of 316 L stainless steel with a diode pumped solid state laser. J Laser Appl 18:205–209
11. Spiro A, Lowe M, Pasmanik G (2012) Drilling rate of five metals with picosecond laser pulses at 355, 532, and 1064 nm. Appl Phys A 107:801–808
12. Stašić J, Gaković B, Trtica M, Desai T, Volpe L (2012) Superficial changes on the Inconel 600 superalloy by picosecond Nd:YAG laser operating at 1064, 532, and 266 nm: comparative study. Laser Part Beams 30:249–257
13. Wang WJ, Mei XS, Jiang GD (2009) Control of microstructure shape and morphology in femtosecond laser ablation of imprint rollers. Int J Adv Manuf Technol 41:504–512
14. Döring S, Richter S, Tünnermann A, Nolte S (2011) Evolution of hole depth and shape in ultrashort pulse deep drilling in silicon. Appl Phys A 105:69–74
15. Döring S, Ullsperger T, Heisler F, Richter S, Tünnermann A, Nolte S (2013) Hole formation process in ultrashort pulse laser percussion drilling. Phys Procedia 41:431–440
16. Pandey ND, Shan HS, Bharti A (2006) Percussion drilling with laser: hole completion criterion. Int J Adv Manuf Technol 28: 863–868
17. Walther K, Brajdic M, Kreutz EW (2008) Enhanced processing speed in laser drilling of stainless steel by spatially and temporally superposed pulsed Nd:YAG laser radiation. Int J Adv Manuf Technol 35:895–899
18. Jahns D, Kaszemeikat T, Mueller N, Ashkenasi D, Dietrich R, Eichler HJ (2013) Laser trepanning of stainless steel. Phys Procedia 41:630–635
19. Chien WT, Hou SC (2007) Investigating the recast layer formed during the laser trepan drilling of Inconel 718 using the Taguchi method. Int J Adv Manuf Technol 33:308–316
20. Foehl C, Breitling D, Jasper K, Radtke J, Dausinger F (2002) Precision drilling of metals and ceramics with short and ultrashort pulsed solid state lasers. Proc SPIE 4426:104–107
21. Dhar S, Saini N, Purohit R (2006) A review on laser drilling and its techniques. Proc Int Conf Adv Mech Eng 1–3
22. Bonse J, Wrobel JM, Krüger J, Kautek W (2001) Ultra short-pulse laser ablation of indium phosphide in air. Appl Phys A 72:89–94
23. Liu JM (1982) Simple technique for measurements of pulsed Gaussian-beam spot sizes. Opt Lett 7:196–198
24. Semaltianos NG, Perrie W, French P, Sharp M, Dearden G, Logothetidis S, Watkins KG (2009) Femtosecond laser ablation characteristics of nickel-based super alloy C263. Appl Phys A 94: 999–1009
25. Wang WJ, Mei XS, Jiang GD, Lei ST, Yang CJ (2008) Effect of two typical focus positions on microstructure shape and morphology in femtosecond laser multi-pulse ablation of metals. Appl Surf Sci 255:2303–2311
26. Dausinger F (2000) Precise drilling with short pulsed lasers. Proc SPIE 3888:180–187
27. Döring S, Richtera S, Nolte S, Tünnermann A (2011) In-situ observation of the hole formation during deep drilling with ultrashort laser pulses. Proc SPIE 7925:792517–1–8
28. König J (2005) Plasma evolution during metal ablation with ultrashort laser pulses. Opt Express 13:10597–10607
29. Russo RE, Mao XL, Liu HC, Yoo JH, Mao SS (1999) Time-resolved plasma diagnostics and mass removal during single-pulse laser ablation. Appl Phys A 69:S887–S894
30. Mao SS, Mao X, Greif R, Russo RE (2000) Initiation of an early-stage plasma during picosecond laser ablation of solids. Appl Phys Lett 77:2464–2466
31. Račiukaitis G, Brikas M, Gečys P, Voisiat B, Gedvilas M (2009) Use of high repetition rate and high power lasers in microfabrication: how to keep the efficiency high? J Laser Micro Nanoeng 4:186–191
32. Kononenko TV, Klimentov SM, Garnov SV, Konov VI, Breitling D, Föhl C, Ruf A, Radtke J, Dausinger F (2002) Hole formation process in laser deep drilling with short and ultrashort pulses. Proc SPIE 4426:108–112
33. Utéza O, Sanner N, Chimier B, Brocas A, Varkentina N, Sentis M, Lassonde P, Légaré F, Kieffer JC (2011) Control of material removal of fused silica with single pulses of few optical cycles to sub-picosecond duration. Appl Phys A 105:131–141
34. Breitling D, Ruf A, Dausinger F (2004) Fundamental aspects in machining of metals with short and ultrashort laser pulses. Proc SPIE 5339:49–63
35. Zhao WQ, Wang WJ, Mei XS, Jiang GD, Liu B (2014) Investigations of morphological features of picosecond dual-wavelength laser ablation of stainless steel. Opt Laser Technol 58:94–99
36. Föhl C, Dausinger F (2003) High precision deep drilling with ultrashort pulses. Proc SPIE 5063:346–351
37. Breitling D, Föhl C, Dausinger F, Kononenko T, Konov V (2004) Drilling of metals, femtosecond technology for technical and medical applications. Top Appl Phys 96:131–156
38. Modest MF (2006) Effects of multiple reflections on hole formation during short-pulsed laser drilling. J Heat Transf 128:653–661
39. Ruf A, Berger P, Dausinger F, Hügel H (2001) Analytical investigations on geometrical influences on laser drilling. J Phys D Appl Phys 34:2918–2925
40. Klimentov SM, Kononenko TV, Pivovarov PA, Garnov SV, Konov VI, Breitling D, Dausinger F (2003) Role of gas environment in the process of deep hole drilling by ultra-short laser pulses. Proc SPIE 4830:515–520